J. Synchrotron Rad. (2000). **7**, 121–130

Recent trends of insertion-device technology for X-ray sources

Hideo Kitamura

Harima Institute, RIKEN, SPring-8, 1-1-1 Kouto, Mikazuki-cho, Sayo-gun, Hyogo 679-5148, Japan. E-mail: kitamura@spring8.or.jp

(*Received 4 February 2000; accepted 23 February 2000*)

As a consequence of the developments of in-vacuum undulators, where permanent magnet arrays are located in an ultrahigh vacuum, the in-vacuum mini-gap undulator with very short period has been successful in the X-ray ring of NSLS in collaboration with SPring-8, producing a new concept for synchrotron radiation facilities. The key feature of the concept is the combination of in-vacuum mini-gap undulators and a low-emittance ring with moderate beam energy. In other words there are possibilities for the design of a moderate-cost medium-sized synchrotron radiation facility, the performance of which may be comparable with that of the existing large-scale facilities. Here the performance of in-vacuum undulators is described, particularly of the mini-gap type. Also described is the essence of the new concept for synchrotron radiation facilities, the so-called new third-generation light source.

Keywords: insertion devices; undulators.

1. Introduction

In the past eight years the three large-scale facilities, ESRF, APS and SPring-8, dedicated to the utilization of synchrotron radiation in the X-ray region have come into routine operation and striking scientific results have been obtained, confirming that the concept of third-generation sources is the best solution for promoting present and future synchrotron radiation science. As a result, demands for X-ray beamlines have become much stronger in many research fields, particularly biological science. Taking prospective demands in medical or industrial applications into account, each country may have an X-ray facility to meet them and domestic/urgent requirements. Nowadays, however, it is unrealistic that we should wish for other large-scale facilities with beam energies higher than 6 GeV because the construction cost may exceed $500M, too high for an individual country. A reasonable beam energy for such a facility may probably be less than 3.5 GeV. Therefore it may be very difficult to obtain high brightness in the X-ray region by using ordinary undulators designed under the conventional concept where wigglers are preferred for obtaining high-energy radiation, which means that one cannot benefit from high-brilliance X-rays, good spatial coherence or various polarizations without using one of the three large-scale facilities. Recently, however, the situation has drastically changed. As a consequence of the developments of in-vacuum undulators, where the permanent magnet arrays are located in an ultrahigh vacuum (Kitamura, 1998), a special undulator with a very short period, a so-called mini-gap undulator, has been successful in the X-ray ring of NSLS in collaboration with SPring-8 (Stefan *et al.*, 1998), which has produced a new concept for synchrotron radiation facilities. The key feature of the concept is the combination of in-vacuum mini-gap undulators and a low-emittance ring with moderate beam energy. In other words there are possibilities for the design of a moderate-cost medium-sized synchrotron radiation facility, the performance of which may be comparable with that of the existing large-scale facilities. In this paper we describe the performance of in-vacuum undulators, particularly of the mini-gap type, and the essence of the new concept for synchrotron radiation facilities, the so-called new third-generation light source.

2. General performance of undulator radiation

In order to understand the importance of undulator radiation, its performance is compared with that of bending-magnet and wiggler sources. In the comparison, E_B is denoted as the beam energy (GeV), I_B is the beam current (A), B is the magnetic field (T), $\varepsilon_x/\varepsilon_y$ is the emittance, σ_x/σ_y is the beam size, $\sigma_{x'}/\sigma_{y'}$ is the beam divergence and β_x/β_y is the betatron function in the horizontal/vertical direction. In most cases, at the center of an insertion device the following relations involving the above beam parameters apply,

$$\sigma_{x,y} = (\beta_{x,y}\varepsilon_{x,y})^{1/2}, \qquad \sigma_{x',y'} = (\varepsilon_{x,y}/\beta_{x,y})^{1/2}. \qquad (1)$$

2.1. *Bending-magnet source*

Fig. 1 shows a schematic illustration of a typical bending-magnet source. This source is composed of many small

light-source units, so that we can say that this source is a multimode source in the transverse plane. The opening angle of each unit source is approximated as

$$\sigma_{r'} \simeq 13(\lambda E_B/\rho)^{1/2}, \quad (2)$$

where λ is the wavelength and ρ is the radius of the electron orbit (Green, 1976). To obtain coherent radiation we have to extract a single source unit using a spatial filter. As a result, we must lose most of the flux. The degradation of the intensity by a finite emittance of the stored beam is not so drastic since the bending-magnet source is inherently divergent in the horizontal direction.

The other feature of this radiation is that the spectrum is continuous in the wide photon energy range up to the X-ray region and characterized by the critical photon energy given by

$$\varepsilon_c = 665\, E_B{}^2 B \quad \text{(eV)}. \quad (3)$$

The spectral photon flux density is given by

$$D_{\text{bend}} = \frac{1.325 \times 10^{13}}{f_D} G(\varepsilon/\varepsilon_c) E_B{}^2 I_B \left[\text{photons s}^{-1}\ \text{mrad}^{-2}\ (0.1\%\ \text{bandwidth})^{-1}\right]. \quad (4)$$

Here the spectral function, G, is given by

$$G(u) = \left[uK_{2/3}(u/2)\right]^2, \quad (5)$$

where $K_{2/3}$ is the modified Bessel function. Since the deflection angle of the bending magnet is much larger than the horizontal beam divergence, the degradation factor, f_D, is given by

$$f_D = \left(1 + \sigma_{y'}^2/\sigma_{r'}^2\right)^{1/2}. \quad (6)$$

In most cases, $\sigma_{r'}$ is much larger than $\sigma_{y'}$. In the case of SPring-8 (E_B = 8 GeV, ρ = 39.3 m), for example, $\sigma_{r'}$ for λ = 1 Å is calculated as 60 μrad, much larger than the vertical beam divergence of 0.6 μrad. As predicted before, therefore, we may treat f_D practically as unity. The function G has a maximum value of 1.45 at $\varepsilon = \varepsilon_c$. When the magnetic field of the bending magnet is assumed to be 1 T, we obtain approximately the maximum flux density at ε_c = $665\, E_B{}^2$ (eV),

$$(D_{\text{bend}})_{\max} = 1.92 \times 10^{13} E_B{}^2 I_B \left[\text{photons s}^{-1}\ \text{mrad}^{-2}\ (0.1\%\ \text{bandwidth})^{-1}\right]. \quad (7)$$

2.2. *Wigglers*

A wiggler is a type of insertion device. As shown in Fig. 2, this device is composed of many bending magnets having opposite polarities. Therefore the electron shows a wiggle motion, and the intensity of radiation is obtained by multiplying by the number of magnets. In a similar way the spectral flux density of the wiggler radiation is obtained by multiplying that of the bending-magnet source by the number of poles,

$$D_{\text{wiggler}} = \frac{1.325 \times 10^{13}}{f_D} G(\varepsilon/\varepsilon_c) E_B{}^2 I_B\, 2N \left[\text{photons s}^{-1}\ \text{mrad}^{-2}\ (0.1\%\ \text{bandwidth})^{-1}\right], \quad (8)$$

where N is the number of periods. To compare the performance of wiggler radiation with that of the bending-magnet source, we assume a 2 T wiggler having a total length of 4 m. When the magnetic gap is assumed to be 20 mm, the minimum period length to obtain a magnetic field of 2 T is estimated to be about 12 cm. As a result, the total number of periods is 38, so the maximum flux density of wiggler radiation at $\varepsilon_c = 1330\, E_B{}^2$ (eV) is

$$(D_{\text{wiggler}})_{\max} = 1.27 \times 10^{15} E_B{}^2 I_B \left[\text{photons s}^{-1}\ \text{mrad}^{-2}\ (0.1\%\ \text{bandwidth})^{-1}\right], \quad (9)$$

where the factor f_D is also assumed to be unity.

2.3. *Undulators*

An undulator is the other type of insertion device (Alferov *et al.*, 1974). Similarly to a wiggler, this device is composed of many magnets as shown in Fig. 3. However, the magnetic field is relatively low compared with the wiggler case. Therefore the deflection angle, ψ_0, in the undulator is very small, *e.g.* the inverse of the Lorentz factor γ. The angle ψ_0 is given by $K\gamma$. The factor K is the deflection parameter, which is proportional to the magnetic field as

$$K = 93.4\, B\, \lambda_u, \quad (10)$$

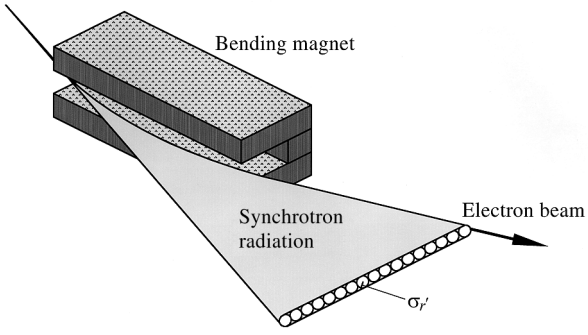

Figure 1
Principle of a bending-magnet source.

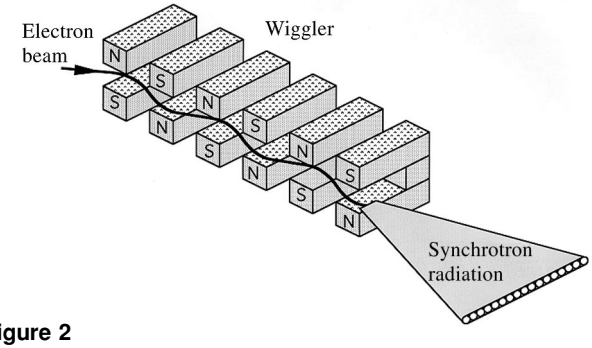

Figure 2
Principle of a wiggler source.

where λ_u is the periodic length of the undulator in metres. Owing to interference effects, a quasi-monochromatic radiation in the shape of a single cone is radiated. The opening angle of the radiation is given by

$$\sigma_{r'} = (\lambda/L)^{1/2}, \tag{11}$$

where λ is the wavelength of the central radiation and L is the device length (Attwood *et al.*, 1985). Generally, the radiation is accompanied by higher harmonics. Different from the bending-magnet radiation, the opening angle $\sigma_{r'}$ is very small in both horizontal and vertical directions. The nth harmonic is obtained at the photon energy as

$$\varepsilon_n = 9.50\, nE_B{}^2/[\lambda_u(1 + K^2/2)] \quad \text{(eV)}. \tag{12}$$

Using (10), (12) can be rewritten as

$$\varepsilon_n = 887\, nBE_B{}^2/[K(1 + K^2/2)] \quad \text{(eV)}. \tag{13}$$

When the beam energy is given, high-energy undulator radiation can be obtained by applying a high magnetic field while keeping K low. However, it should be noted that the spectral intensity depends strongly on the K value. The flux density is proportional to the square of the number of periods,

$$D_{\text{undulator}}(\varepsilon_n) = \frac{1.74 \times 10^{14}}{f_D} N^2 F_n(K) E_B{}^2 I_B \left[\text{photons s}^{-1}\ \text{mrad}^{-2}\ (0.1\%\ \text{bandwidth})^{-1}\right]. \tag{14}$$

In the above equation, F_n is the spectral function for the nth higher order,

$$F_n(K) = K^2\xi^2\left[J_{(n+1)/2}(K^2\xi/4) - J_{(n-1)/2}(K^2\xi/4)\right]^2, \qquad \xi = n/(1 + K^2/2), \tag{15}$$

where J_i is the Bessel function. When $K << 1$, the function F_1 for the fundamental is proportional to K^2 and has a maximum of 0.38 at $K = 1.2$, which is an optimum K value for obtaining the highest intensity of the fundamental. At that K value, other higher harmonics show $F_3 = 0.28$, $F_5 = 0.13$, $F_7 = 0.051$, $F_9 = 0.019$ and $F_{11} = 0.0069$. The degradation factor for undulator radiation is given by

$$f_D = \left[\left(1 + \sigma_{x'}^2/\sigma_{r'}^2\right)\left(1 + \sigma_{y'}^2/\sigma_{r'}^2\right)\right]^{1/2}. \tag{16}$$

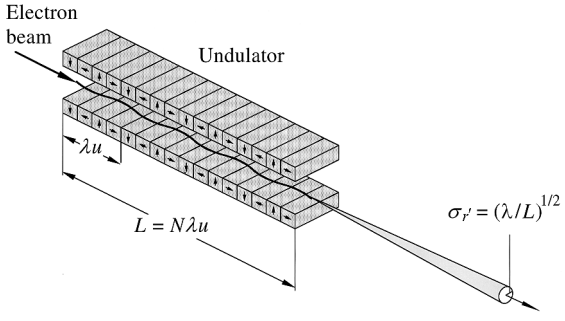

Figure 3
Principle of an undulator source.

In the X-ray region, f_D might be much higher than unity even if a third-generation source were considered. In the case of SPring-8 ($L = 4.5$ m), for example, $\sigma_{r'}$ for $\lambda = 1$ Å is very small, *i.e.* 5 μrad, while the horizontal/vertical beam divergence is 19 μrad/0.9 μrad, giving $f_D = 3.9$.

To compare the spectral performance of the undulator radiation with that of the other sources we assume a short-period undulator ($\lambda_u = 13$ mm) having a total length of 2 m ($N = 153$). A magnetic field of 1 T, corresponding to $K = 1.2$, can be obtained at a gap of 3 mm, which is not difficult to achieve since in-vacuum undulator technology is available at present. The fundamental is obtained at $\varepsilon_1 = 506E_B{}^2$, near the critical energy of the bending-magnet radiation. The spectral intensity is calculated as

$$D_{\text{undulator}}(\varepsilon_1) = \frac{1.55 \times 10^{18}}{f_D} E_B{}^2 I_B \left[\text{photons s}^{-1}\ \text{mrad}^{-2}\ (0.1\%\ \text{bandwidth})^{-1}\right]. \tag{17}$$

In addition, the third harmonic is obtained at $\varepsilon_3 = 1520E_B{}^2$ near the critical energy of the wiggler radiation. The intensity is also calculated as

$$D_{\text{undulator}}(\varepsilon_3) = \frac{1.14 \times 10^{18}}{f_D} E_B{}^2 I_B \left[\text{photons s}^{-1}\ \text{mrad}^{-2}\ (0.1\%\ \text{bandwidth})^{-1}\right]. \tag{18}$$

If the beam emittance were zero ($f_D = 1$), the spectral intensity of the undulator radiation would be by five or three orders higher than that of the bending magnet or wiggler, respectively. In the case of actual storage rings, however, the emittance is finite, which means that the above performance can no longer be expected.

To make comparisons of these three sources for various emittances, *i.e.* $\varepsilon = 0$, 3, 30, 300 nm rad, we assume a beam energy of 3 GeV and an emittance coupling of 1%. The device parameters assumed here are the same as those adopted in the preceding paragraph. The result of the comparison is shown in Fig. 4. In the case of the undulator, the reduction of the intensity by the finite emittance effect is found to be drastic, particularly for higher harmonics, while the intensity of the bending-magnet or wiggler radiation is not affected. Nevertheless, if a very low emittance of 3 nm rad is possible, we can obtain an X-ray intensity higher by two to three orders than that of the wiggler. In the above discussion the degradation effect by energy spread in the stored beam or error fields of undulator magnets (Walker, 1993) is not considered. These effects are serious when much higher harmonics are used.

3. In-vacuum undulator technology

For undulator design relating to vacuum chambers we can adopt two types: out-of-vacuum and in-vacuum, as shown in Fig. 5. In the case of the out-of-vacuum type, the advantages are that the handling of the permanent magnets is very easy and the vacuum system can be fabricated independently from the other parts of the device. Therefore

most of the existing undulators are of the out-of-vacuum type. The disadvantages are that the thickness of the chamber wall is not negligible in the case of short-period undulators since a very short magnetic gap is required for such undulators. Also, we have to adopt a conservative gap value since the inner height of the chamber should include a margin for injection or unordinary operation of the storage ring. Therefore, the magnetic gap may be too wide to realize short-period undulators.

On the other hand, the in-vacuum type is the most suitable for short-period undulators. The permanent magnets are arranged in the same ultrahigh vacuum as for a storage ring, so that the vacuum gap is equal to the magnetic gap. Therefore this type has a great flexibility for any operation of the ring. For example, for injection or unordinary operation the gap can be set at a wide value, and for user operation the gap can be closed down to the required value. The disadvantages are that it is difficult to construct because we have to realize ultrahigh vacuum (UHV) without any demagnetization of the undulator magnets, and the fabrication of the vacuum system cannot be separated from the other parts of the device.

The first in-vacuum undulator was developed at KEK (Yamamoto *et al.*, 1992). This device was installed in the 6.5 GeV accumulation ring, which was a storage-ring-type injector for the 30 GeV Tristan Main Ring; the operation of this ring was terminated in 1995. The period length of the undulator is of the order of 4 cm, which can be realized with ordinary out-of-vacuum-type undulators. The most important reason for adopting in-vacuum-type undulators was to keep the performance of the storage ring as an injector. When the ring was operated as an injector for the Main Ring, the gap could be opened up to 50 mm.

The key point in terms of the technology is that the delicate undulator magnet system should be compatible with UHV. There are several difficulties, but we have solutions. (i) To reduce outgassing from permanent magnets having a porous structure, the magnets should be coated with TiN. (ii) To avoid demagnetization due to UHV bakeout we have to adopt special permanent magnets with very high coercivity at high temperature. (iii) In the UHV, cement or glue cannot be used so we have to adopt a mechanical clamping method. (iv) The magnet surface of the gap side should be smooth to reduce the production of a wake field induced by a strongly bunched beam (Hara, Tanaka, Tanabe, Marechal, Kitamura *et al.*, 1998), so we cannot adopt the shimming method of putting steel foil onto the magnet surface. To correct the magnetic field we have to insert small magnet chips on the back of the magnet.

At SPring-8 the full-scale adoption of in-vacuum-type undulators has been made. At present, 14 in-vacuum undulators of various types have been installed in the 8 GeV storage ring. In the following we describe the brief features of the devices, which are summarized in Table 1.

Standard in-vacuum X-ray undulators. Most of the X-ray applications populate the photon energy region from 8 keV to 16 keV. To meet the above requirement we have constructed nine in-vacuum undulators having the same design. Therefore they are called standard in-vacuum X-ray undulators. The undulator magnet array is composed of NdFeB permanent magnets with a period length of 32 mm, 140 periods and a maximum field of 0.85 T at a minimum gap of 8 mm. To obtain compatibility with UHV the permanent magnets, having high coercivity, are coated with TiN (Hara, Tanake, Tanabe, Marechal, Okada & Kitamura, 1998). With a beam energy of 8 GeV, the fundamental of the radiation can cover the energy range from 5 keV to 18 keV, and higher harmonics up to the fifth can cover the range up to 80 keV. Fig. 6 shows one of the standard in-

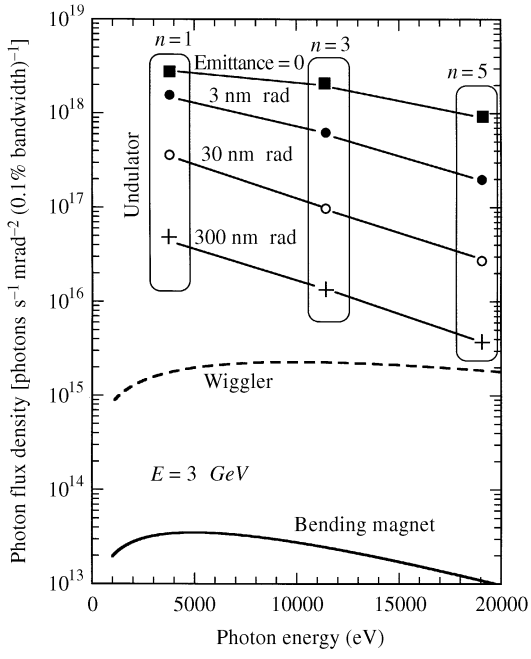

Figure 4
Spectral comparison among bending-magnet, wiggler and undulator sources for various emittances ε = 0, 3, 30, 300 nm rad with a coupling of 1%. The beam energy is assumed to be 3 GeV.

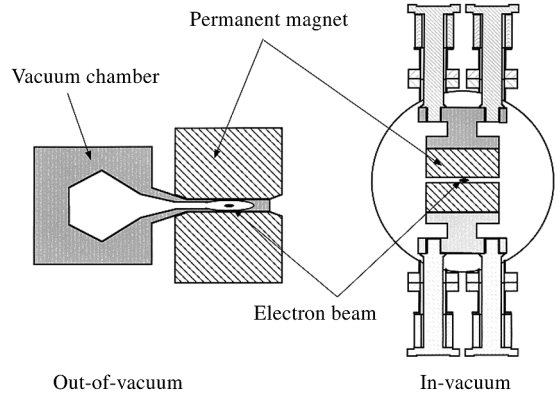

Figure 5
Schematic illustration of two possible designs of the vacuum system for undulators.

Table 1
In-vacuum undulators at SPring-8 (Summer 1999).

P_T and P_D denote the total radiated power and power density, respectively.

In-vacuum undulator	λ_u (mm)	N	G_{min} (mm)	B_{max} (T)	K	Polarization	$n = 1$ (keV)	$n = 3$ (keV)	$n = 5$ (keV)	P_T (kW)	P_D (kW mrad^{-2})	Total number
Standard X-ray	32	140	8	0.87	2.6	Horizontal	4.3–18.5	13–51	22–75	13.7	525	9
Industrial	40	112	12	0.70	2.6	Horizontal	3.6–14.5	11–40	18–60	8.5	306	1
Hybrid	24	187	5	1.16	2.6	Horizontal	5.8–25	18–70	30–100	24.3	870	1
Tandem vertical	37	2 × 37	8	0.5	1.7	Vertical	6.7–16	20–40	33–70	1.37	70	1
Figure-8	26, 52	172, 86	5	0.99, 0.30	2.4, 1.45	Horizontal, vertical	4.76–20			18.9	186	1
Helical	36	125	7	0.33	1.1	Circular	7.6–16.5			4.0	79	1

vacuum X-ray undulators installed in the straight section of SPring-8.

In-vacuum undulator for industrial applications. To extend the available photon energy down to 4 keV, we constructed an undulator having a period length of 40 mm, somewhat longer than that of the standard type.

In-vacuum X-ray hybrid undulator. To obtain a high photon energy with the fundamental, we constructed a special in-vacuum undulator of hybrid type composed of NdFeB magnets and permendur poles. The period length is as short as 24 mm so that the fundamental may cover the energy range up to 25 keV. The maximum field can be obtained as 1.1 T at a gap of 5 mm.

In-vacuum tandem vertical undulator. This undulator is composed of two identical units for producing vertically polarized X-rays having different photon energies on the same axis (Tanaka *et al.*, 1998). The periodic length is 37 mm, the number of periods per unit is 37. The attached beamline for structural biology is designed to make the best use of vertical polarization, *e.g.* a diamond monochromator is operated as a beam splitter in the horizontal direction (Yamamoto *et al.*, 1998).

In-vacuum figure-8 undulator. The magnet structure of the figure-8 undulator is shown schematically in Fig. 7. The undulator is composed of six magnet arrays. The outer four magnet arrays generate a horizontal field, the central two arrays generate a vertical field. The period length of the horizontal field is twice as long as that of the vertical field, so that the electron trajectory projected in the transverse plane looks like a figure of 8. Therefore this device is called a figure-8 undulator. Originally, the figure-8 undulator design was developed to obtain a special radiation having a low central power density like that of a helical undulator, which is the most important characteristic of the figure-8 design (Tanaka & Kitamura, 1995). However, this type has another important characteristic: both horizontal and vertical polarizations are available (Tanaka *et al.*, 1998). As shown in Fig. 8, integer/half-odd-integer harmonics are polarized horizontally/vertically.

In-vacuum helical undulator. In some scientific fields one needs only a high photon flux of the radiation with a moderate energy resolution. To meet this requirement we have developed an in-vacuum helical undulator for the X-ray region. The period length is 36 mm, the number of periods is 125. The maximum field of 0.36 T is obtained at a gap of 7 mm. It is well known that the on-axis radiation from helical undulators has no higher harmonic (Kincaid, 1977). Therefore we can obtain a quasi-monochromatic X-ray by using only a spatial filter as shown in Fig. 9, where the spectral flux is calculated for various aperture values of the spatial filter. By making the aperture smaller, the bandwidth of the first harmonic is narrower, as well as the contribution from the higher harmonics being smaller.

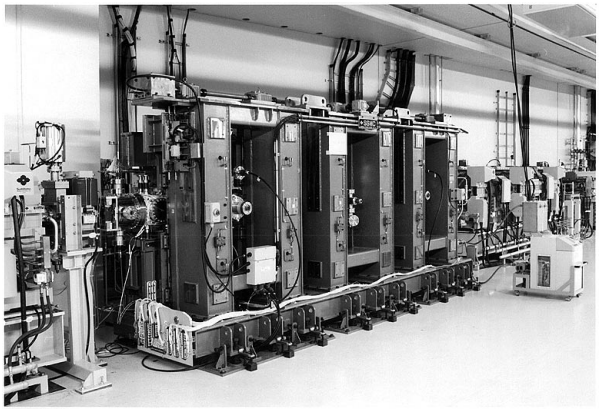

Figure 6
Standard in-vacuum X-ray undulator installed in the straight section of SPring-8.

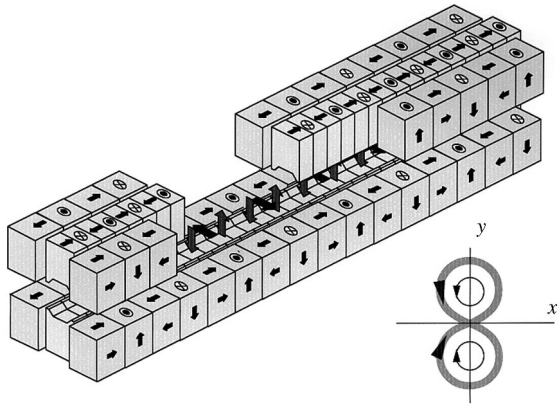

Figure 7
Principle of the figure-8 undulator design. The electron trajectory projected in the transverse plane looks like a figure of 8.

Finally, the relative bandwidth is obtained as 1.5%, which is small enough to perform small-angle scattering experiments in the attached beamline having no monochromator.

The radiation is polarized circularly, which is not important for the purpose of the present beamline. Therefore, the device has no switching system of helicity. It should be noted that variable polarization undulators (Sasaki *et al.*, 1994; Kimura *et al.*, 1996) are very important tools in the soft X-ray region where no good phase retarder is available. In the X-ray region, however, variable polarization can be obtained easily by the combination of a planar undulator and a crystal phase retarder (Suzuki *et al.*, 1998). This system has higher reliability: the system causes no effect on the stored beam, and both right- and left-hand polarizations are obtained on the same axis. In addition, the switching speed of helicity is higher than 40 Hz.

4. In-vacuum mini-gap undulators

To obtain very high photon energy radiation with an undulator, the period length should be as short as possible, which can be realized only by mini-gap undulators with a magnetic gap of less than 5 mm. The key technology for the mini-gap undulators has been developed as an extension of that of in-vacuum undulators. The first mini-gap undulator was constructed as a collaborated work between NSLS and SPring-8. The period length is very short, *i.e.* 11 mm, and the number of periods is 29. The maximum field of 0.7 T ($K = 0.72$) is obtained at the minimum gap of 3.2 mm. The device has been successfully operated in the X-ray ring at NSLS since 1997. Although the beam energy is not as high as 2.58 GeV, the fundamental is obtained at 4.5 keV and the third harmonic at 13.5 keV. Therefore this success has been a strong impact on other light-source projects.

4.1. *Beam lifetime and device length*

We are interested in the small gap limit of the undulator, which is related to the beam lifetime performance in the storage ring. The overall lifetime, τ_O, is given by the partial lifetimes as

$$\tau_O^{-1} = \tau_C^{-1} + \tau_T^{-1} + \tau_B^{-1} + \tau_Q^{-1}, \tag{19}$$

where τ_C is the lifetime related to coulomb scattering by residual gases, τ_T is the Touschek lifetime related to the collision of electrons in the bunch (Bernardini *et al.*, 1963), τ_B is the lifetime related to the energy loss of electrons due to Bremsstrahrung, and τ_Q is the quantum lifetime, being very long in the case of low-emittance rings. If there is an obstacle reducing the aperture for the stored beam, then t_C becomes shorter,

$$\tau_C \propto E_B{}^2 d^2 / (\beta_1 \langle P\beta \rangle), \tag{20}$$

where d is the distance from the centre of the beam to the obstacle, β_1 is the betatron function at the obstacle, P is the pressure, $\langle P\beta \rangle$ is the average value of $P\beta$ along the circumference of the ring. The envelope of the stored beam is proportional to the square root of the betatron function. Therefore the highest loss of the beam occurs at the point where the vertical betatron function, β_y, has a maximum in the undulator. As shown in Fig. 10, if the undulator is located at the symmetry point where the vertical betatron function has a minimum (β_{y0}), it shows a maximum (β_y) at both ends of the undulator,

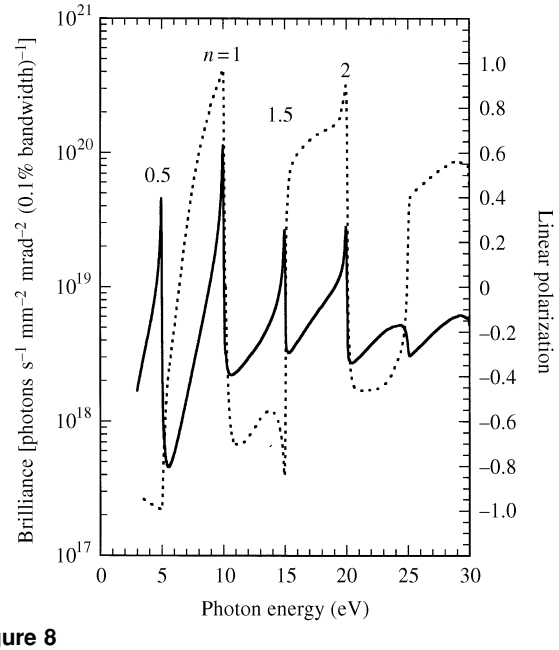

Figure 8
Spectral brilliance (full curve) and polarization (dotted curve) obtained from an in-vacuum figure-8 undulator.

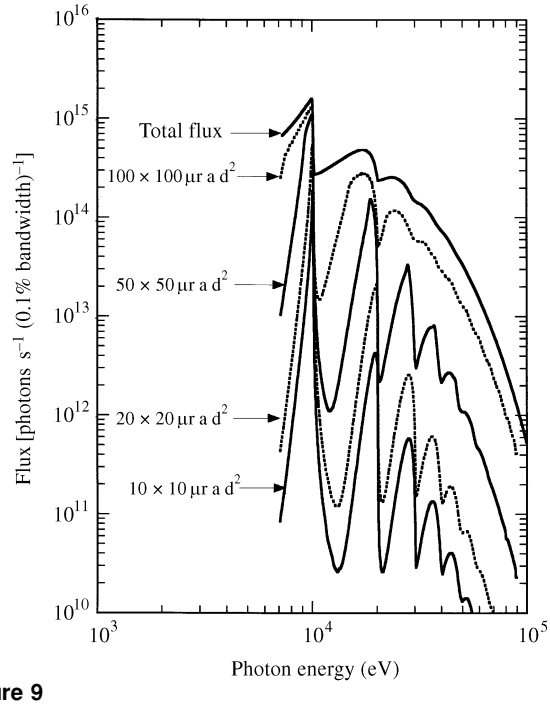

Figure 9
Spectral flux obtained from an in-vacuum helical undulator (λ_u = 3.6 cm, $N = 125$, $K = 0.83$) for various apertures of spatial filter.

$$\beta_y = \beta_{y0} + \left[(L/2)^2/\beta_{y0}\right], \tag{21}$$

where L is the length of the undulator. From this equation the minimum value of β_y is found to be L when $\beta_{y0} = L/2$, which gives the longest beam lifetime when the undulator length is given. If β_{y0} is optimized to be $L/2$ for the undulator with gap value G, (20) can be rewritten by substituting L for β_1 as

$$\tau_C \propto {E_B}^2 G^2/\left(L\langle P\beta\rangle\right). \tag{22}$$

In the case of mini-gap undulators, therefore, the undulator length should be made short to keep the lifetime reasonably long, and the vertical betatron function should be optimized to be half of the undulator length. For example, G = 8 mm and L = 4 m gives the same lifetime as for G = 4 mm and L = 1 m. Nevertheless, the number of periods is still large since the period length is very short, which may give radiation of high intensity.

In any case it is desirable to obtain a long beam lifetime, not only for performing reliable synchrotron radiation experiments but also to avoid demagnetization of the permanent magnets due to electron beam loss on them. Such demagnetization may cause a phase error in undulator magnets, which may reduce the intensity of the undulator radiation, particularly the intensities of higher harmonics. Therefore the undulator gap should be set at the smallest value which does not reduce the beam lifetime. At SPring-8 the minimum gap for the 4.5 m device is set at 8 mm; however, we have not observed any reduction of the spectral intensity of the fifth harmonic after three years of operation

It should be noted that τ_C is very short for low E_B as shown in equation (22). Therefore, in the case of low-energy rings where mini-gap undulators may be greatly desired, it is necessary to design a special ring vacuum system able to perform in the 10^{-9} Pa range; this pressure is by an order as low as that of an ordinary storage ring. In addition, there is another difficulty with low-energy rings; the Touschek lifetime, τ_T, is very short since it is approximately proportional to ${E_B}^3$ if the bunch volume is given. This difficulty is more serious for low-emittance rings where the electron density in the bunch is very high. At present there is no effective solution without degrading the performance of the electron beam.

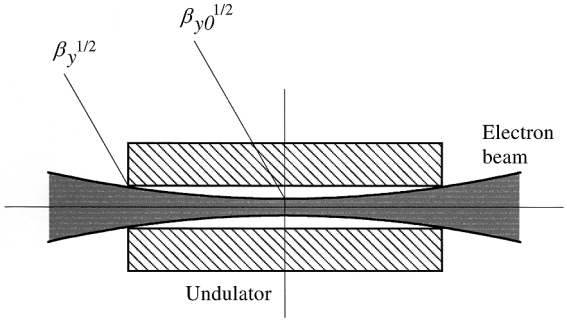

Figure 10
Example of a beam envelope at an undulator location. The amplitude of the envelope is proportional to the square root of the betatron function.

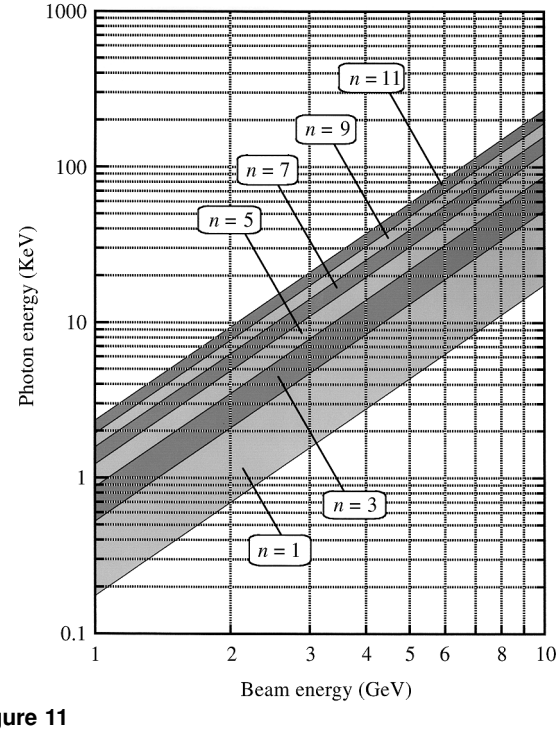

Figure 11
Example of the tunable range in the single-undulator concept. The period length is assumed to be 18 mm and the minimum gap 3 mm.

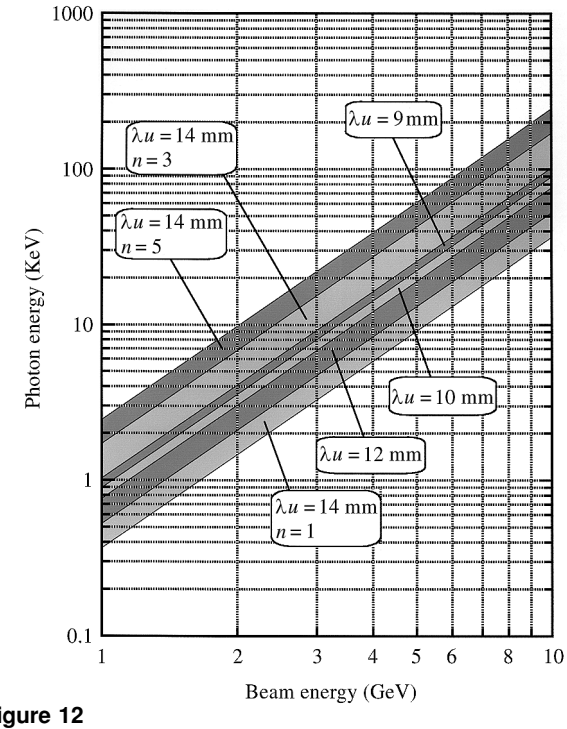

Figure 12
Example of the tunable range in the multi-undulator concept. The undulator has four magnet arrays with period lengths of 9, 10, 12, 14 mm. The minimum gap of each array is assumed to be 3 mm.

As described in the preceding paragraph, the device length of a mini-gap undulator is desired to be short, as well as the vertical betatron function at the location of the device being designed to be very small. This means that the vertical beam divergence becomes large unless the vertical emittance is made very low. In other words the performance of very low emittance coupling is necessary for obtaining a high brilliance of undulator radiation.

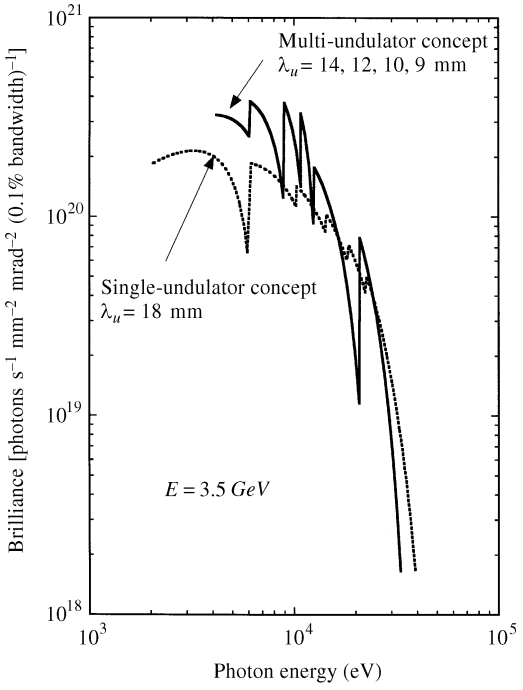

Figure 13
Comparison of spectral brilliances between single-undulator (dotted curve) and multi-undulator (full curve) concepts. The beam energy is assumed to be 3.5 GeV, emittance 3 nm rad, emittance coupling 1%, undulator length 1.5 m, and minimum gap 3 mm.

4.2. *Tunability*

Generally the tunable energy range of short-period undulators is narrow since the maximum K value is not so high. There are two approaches to expand the available range. The first one, the single-undulator concept, is to use a single undulator having a relatively long period for obtaining a high K value. As a matter of course, the energy of the fundamental is made lower inevitably down to the soft X-ray region. However, we can obtain X-ray radiation by using higher harmonics, *e.g.* the seventh, ninth or eleventh. The other approach is a multi-undulator concept where we can tune the photon energy in the wide range by selecting one of the several undulator magnet arrays having a different period length. Although the tunability of each array is narrow, we can obtain wide tunability of the whole system (Kitamura, 1995).

Fig. 11 shows an example of the tunable range of a mini-gap undulator in the single-undulator concept. The period length is assumed to be 18 mm so that the maximum K value may exceed a value of 2 at a gap of 3 mm, which means that the tunable ranges of the first and third harmonics overlap each other. If we use higher harmonics, up to the eleventh, we obtain a tunable range from 1 keV to 15 keV for 2.5 GeV, and from 2 keV to 30 keV for 3.5 GeV. Fig. 12 shows the results in the multi-undulator concept. For example, the multi-undulator has four magnet arrays

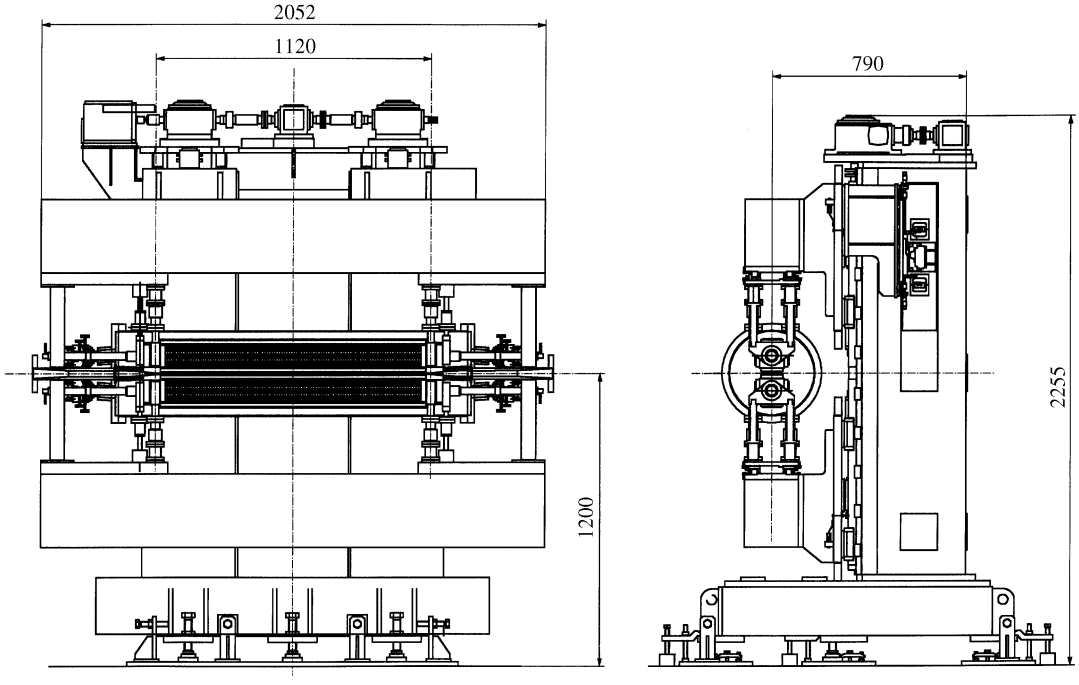

Figure 14
Plan view of the in-vacuum mini-gap revolver undulator under construction at SPring-8.

with period lengths 14 mm, 12 mm, 10 mm and 9 mm, and the minimum gap of each array is assumed to be 3 mm. For the 14 mm array we use higher harmonics up to the fifth. For the other arrays we use only the fundamental. We obtain a tunable range from 2 keV to 15 keV for 2.5 GeV, and from 4 keV to 30 keV for 3.5 GeV. As a matter of course, to obtain a much wider tunable range we can make use of designs having more arrays, *e.g.* six-array or eight-array systems.

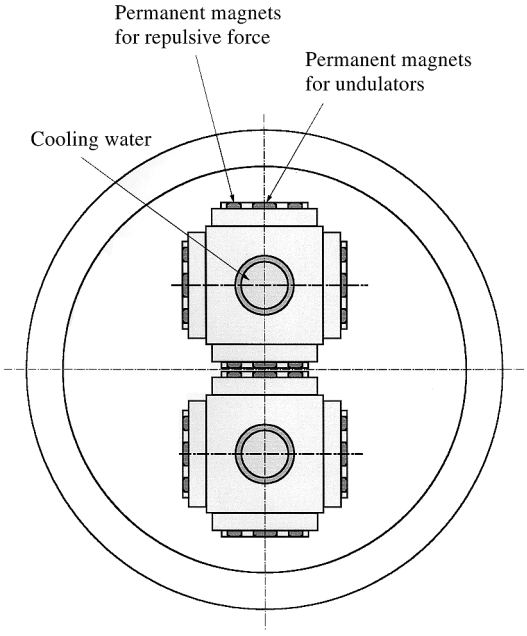

Figure 15
Cross-sectional view of the in-vacuum mini-gap revolver undulator. Dimensions in mm.

In Fig. 13 the spectral brilliances between the two concepts are compared numerically. The beam energy is assumed to be 3.5 GeV, the emittance 3 nm rad, the emittance coupling 1%, the undulator length 1.5 m and the minimum gap 3 mm. The dotted curve shows the case of the single-undulator concept while the full curve shows the case of the multi-undulator concept. The brilliance in the multi-undulator concept is found to be three times as high as that in the single-undulator concept. In the calculation the effect of the energy spread as well as the phase error is not considered. This phase error effect is very serious, particularly in the case of the single-undulator concept where the performance of higher harmonics is important. However, even if we consider these effects, we can obtain a high brilliance of 10^{20} photons s^{-1} mm^{-2} $mrad^{-2}$ (0.1% bandwidth)$^{-1}$ in the X-ray region. This performance may be comparable with that of the existing large-scale facilities.

4.3. *In-vacuum revolver undulator of mini-gap type*

At SPring-8 we are constructing a mini-gap-type multi-undulator for R&D, the so-called in-vacuum mini-gap revolver. Fig. 14 shows a plan view of the device with four different undulator magnet arrays. The total length of each array is 1 m and the period lengths (number of periods) are 6 mm (133), 10 mm (100), 15 mm (66) or 20 mm (50). As shown in Fig. 15, magnet arrays are mounted on the rotating beams, which have water-cooling channels to protect against heating by image beam current (Bane & Krinsky, 1993) or synchrotron radiation from the upstream bending magnet. In the design of the revolver-type undulator, different from ordinary undulators the magnet arrays are supported by bearings at both ends of the beam. Obviously this supporting position is not optimum for minimizing the bend due to the magnetic attractive force, which may give a large flexion in the beam. To reduce such

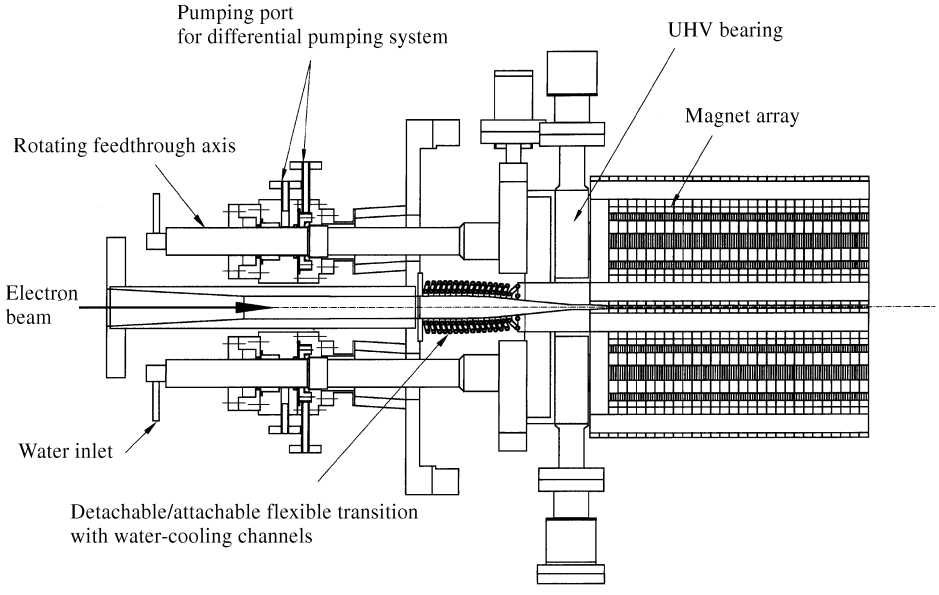

Figure 16
The most important part of the in-vacuum mini-gap revolver undulator.

a flexion, each undulator array has extra magnet arrays on both sides, which gives a repulsive force and works as a magnetic spring. Fig. 16 shows the most important part: rotating feedthrough axes with a two-stage differential pumping system and a detachable/attachable flexible transition with water-cooling channels.

5. Concept of new third-generation light sources

The existing large-scale light sources were planned in the 1980s when the minimum gap of undulators was believed to be about 20 mm; this gap value is small enough to obtain a field of 0.5 T with an undulator having a period length of 40 mm which corresponds to the X-ray region with a beam energy of 6–8 GeV. Nowadays, however, we can utilize in-vacuum mini-gap undulators with a gap of 3 mm, which reduces the possible period length by a factor of about four. As a result we can obtain undulator radiation with an equivalent X-ray performance even if the beam energy is as moderate as 3–4 GeV. In other words there are possibilities for the design of a moderate-cost and medium-sized synchrotron radiation facility, the performance of which may be comparable with that of the existing large-scale facilities; this is the concept of new third-generation light sources. The specifications required for such sources are summarized hereinafter.

As shown in Fig. 4, the emittance should be designed to be less than 10 nm rad for obtaining high-brilliance undulator radiation. In addition, the emittance coupling should be as small as possible, *e.g.* less than 1%. The vertical betatron function at the location of an undulator should be designed to be half of the undulator length, which may be different for each device. Therefore, this function should be variable if possible. As shown in Figs. 11 and 12, the beam energy, E_B, is required to be higher than 2.5 GeV for obtaining undulator radiation in the X-ray region above 10 keV. Nevertheless, E_B is desired to be as high as possible for obtaining a long beam lifetime, as well as the average pressure in the ring being required to be in the 10^{-9} Pa range to reduce the beam loss related to coulomb scattering by residual gases.

The author would like to acknowledge the fruitful discussion with Drs H. Tanaka, T. Tanaka and T. Hara, the staff of SPring-8.

References

Alferov, D. F., Bashmakov, Yu. A. & Bessonov, E. G. (1974). *Sov. Phys. Tech. Phys.* **18**, 1336–1339.
Attwood, D. T., Halbach, K. & Kim, K.-J. (1985). *Science*, **228**, 1265–1272.
Bane, K. & Krinsky, S. (1993). *Proceedings of the 1993 Particle Accelerator Conference*, Washington, DC, USA, pp. 3375–3377. Piscataway, NJ: IEEE.
Bernardini, C., Corazza, G. F., Giugno, G. Di, Ghigo, G., Haissinski, J., Marin, P., Querzoli, R. & Touschek, B. (1963). *Phys. Rev. Lett.* **10**, 407–409.
Green, K. G. (1976). Report 50522. Brookhaven National Laboratory, Upton, NY, USA.
Hara, T., Tanaka, T., Tanabe, T., Marechal, X. M., Kitamura, H., Elleaume, P., Morrison, P., Chavanne, J., Van Vaerenbergh, P. & Schmidt, D. (1998). *J. Synchrotron Rad.* **5**, 406–408.
Hara, T., Tanaka, T., Tanabe, T., Marechal, X. M., Okada, S. & Kitamura, H. (1998). *J. Synchrotron Rad.* **5**, 403–405.
Kimura, S., Kamada, M., Hama, H., Marechal, X. M., Tanaka, T. & Kitamura, H. (1996). *J. Electron Spectrosc. Relat. Phenom.* **80**, 437–440.
Kincaid, B. M. (1977). *J. Appl. Phys.* **48**, 2684–2691.
Kitamura, H. (1995). *Rev. Sci. Instrum.* **66**, 2007–2010.
Kitamura, H. (1998). *J. Synchrotron Rad.* **5**, 184–188.
Sasaki, S., Shimada, T., Yanagida, K., Kobayashi, H. & Miyahara, Y. (1994). *Nucl. Instrum. Methods* A**347**, 87–91.
Stefan, P., Tanabe, T., Krinsky, S., Rakowsky, G., Solomon, L. & Kitamura, H. (1998). *J. Synchrotron Rad.* **5**, 417–419.
Suzuki, M., Kawamura, N., Mizumaki, M., Urata, A., Maruyama, H., Goto, S. & Ishikawa, T. (1998). *Jpn. J. Appl. Phys.* **37**, L1488–1490.
Tanaka, T. & Kitamura, H. (1995). *Nucl. Instrum. Methods*, A**364**, 368–373.
Tanaka, T., Marechal, X. M., Hara, T., Tanabe, T. & Kitamura, H. (1998*a*). *J. Synchrotron Rad.* **5**, 412–413.
Tanaka, T., Marechal, X. M., Hara, T., Tanabe, T. & Kitamura, H. (1998*b*). *J. Synchrotron Rad.* **5**, 414–416.
Walker, R. P. (1993). *Nucl. Instrum. Methods*, A**335**, 328–337.
Yamamoto, M., Kumasaka, T., Fujisawa, T. & Ueki, T. (1998). *J. Synchrotron Rad.* **5**, 222–225.
Yamamoto, S., Shioya, T., Hara, M., Kitamura, H., Zhang, X. W., Mochizuki, T., Sugiyama, H. & Ando, M. (1992). *Rev. Sci Instrum.* **61**, 400–403.